Proceedings of the 5th WSEAS Int. Conf. on Signal Processing, Computational Geometry & Artificial Vision, Malta, September 15-17, 2005 (pp136-142)

Determination of Kinematic Parameters of a Passive Bipedal Walking Robot Moving on a Declined Surface by Image Processing

AHMAD BAGHERI
AMIR HAJILOO
SALAR BASIRI
Department of Mechanical Engineering
University of Guilan,
Po.Box: 3756 – Rasht
IRAN

Abstract: Designing and manufacturing mechanisms that are able to move on a slope according to the gravity has been an issue of the interests of researchers recently. In this paper the designing and manufacturing a Passive biped robot with 3 degrees of freedom is presented. This robot is able to move down on slope with a minimum tangent based on the gravity and without any controller or any supplier. After presenting the governing equations and the dynamic of the robot, a computer simulation is done. Finally a comparison between the results from the physical model and the results from the numerical simulation is done to check the validity of the project.

Key-Words: Passive Biped Robot-Collision Dynamics-Digital Image Processing

1 Introduction

Most terrestrial multi-cellular animals, including humans, can walk. Some people also hope for useful walking robots. Increasing the knowledge of walking has a wide range of applications. Since human motion is controlled by the nervous system and powered by muscles, the role of nerves and muscles is obviously of interest. But one way to understand the role of nerves and muscles is to learn how much can be done without them. Human walking, for example, might be modeled for some purposes as an uncontrolled mechanical process. One idea behind the case is that the role of the nerves and muscles in walking might be more to gently guide than imposingly control. It has been shown by McGeer that stable human-like walking motions can be exhibited by uncontrolled sets of rigid links powered only by gravity [1]. McGeer's work in passive dynamic walking has shown that coordination in human walking does, to some extent, rely on the passive dynamics of the legs. If one's goal is to study active and humanlike robotic walking, it is natural that one would also take advantage of the passive dynamics of the robot's limbs to reduce the energetic and computational cost of coordinating the walker's motion. A simple and open loop powered walking scheme was studied by McGeer (1989, 1990, and 1991).

The approach here was originally pioneered by McGeer (1989-1993), who demonstrated that a two-dimensional, four-link mechanism, which somewhat resembles human legs, is capable of stable, human-like gait down a shallow slope with no activation (besides gravity) and no control. McGeer's passive-dynamic theory of bipedal locomotion describes gait as a natural repetitive motion of a dynamical system or, in the language of nonlinear dynamics, a limit cycle.

2 Passive Walking Mechanism

The two-dimensional kneed walking machine we study here, essentially is a copy of McGeer's design, is shown schematically in Fig.1. It consists of a swing leg (not in contact with the ground) and a stance leg (touching the ground), connected by a frictionless joint at the hip. Extra mass is generally added at the hip serving as a crude model of an upper body. Each leg (assumed identical to the other) is composed of a rigid thigh and shank. The stance knee is locked. For kneed walkers, the swing knee is a frictionless joint with a knee-stop preventing hyperextension between knee strike and heel strike. The knee stop also prevents the stance leg from hyper extending. Straight-legged (knee less) walkers may be viewed as obtained from kneed walkers by permanently locking the knees [6,7].

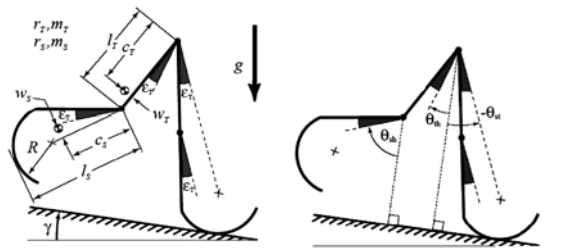

a)Dimensional Parameters b)Dynamic Variables

Fig.1: Description of McGeer's Kneed Walking Model.

The motions of the walker are governed by standard rigid body dynamics. In our way of formulating these, all of the equations described below are based on angular momentum balance about various points. A walking step starts right after heel strike, just when the old stance leg (which is now the swing leg) starts swinging. Equations of motion for the three-link mode are integrated forward in time until knee strike is detected. Assuming no rebound (perfectly plastic knee collision), jump conditions then determine the post-knee strike state. Equations of motion for the two-link mode are now integrated forward in time until heel strike is detected. Assuming no rebound (perfectly plastic heel collision) and no ground impulse at the trailing foot, jump conditions are used to determine the post-heel strike state from the pre-heel strike state.

The state space of this model describes by $\{\theta_{st}, \theta_{th}, \theta_{sh}, \dot{\theta}_{st}, \dot{\theta}_{th}, \dot{\theta}_{sh}\}$, where θ_{st}, θ_{th} and θ_{sh} are stance angle, thigh angle and shank angle, respectively. The simulated walking cycle is shown schematically in Figure (2).

Fig.2: Simulation of Gait Cycle.

After Obtaining of the governing differential equations using the Newton-Euler's, the different collision criteria have been considered. The relation between before and after of the impact has been solved in a forward analysis.

3 Specifications of the Fabricated Biped

The physical characteristics of the fabricated biped are shown in Fig.3. This robot is designed and manufactured based on the McGeer Biped which was first designed and manufactured in Cornell University in the USA [8].

Fig.3: Passive Biped Walker of the University of Guilan

This sort of walkers has 4 legs – 2 couples. The internal couple moves together while the external one does the same so it will prevent the robot from falling asides. Thus it can be assumed as a 2-D Biped walker model with a good approximation**.** Different components of the robot are shown in Fig.4 separately and in detail.

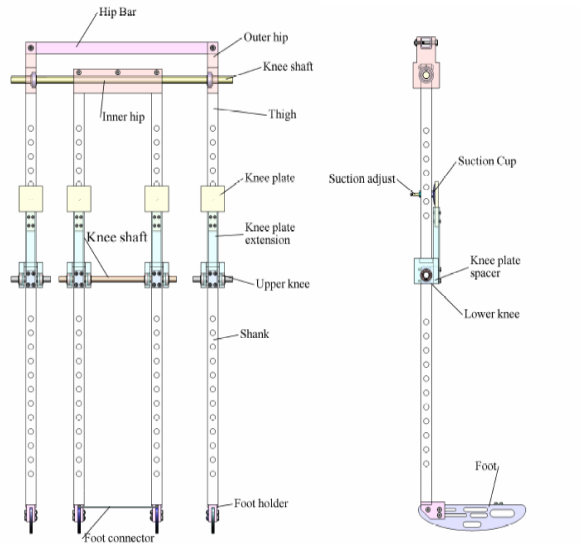

a) Front View b) Left View

Fig. 4: Biped Walker Model in Details

The robot's foot is circular and so it will make an easy rolling contact with the slope. As mentioned before the knee mechanism is one of the important parts of the robot. In this prototype a plane is attached to the knee that is connected to the knee joint in one end. The knee plane is in contact with a suction cup which locks the knee in supporting phase and also prevents the knee from over bending. The knee mechanism is shown in Fig.5.

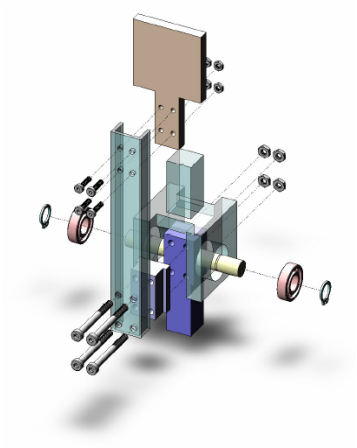

a) Knee joint

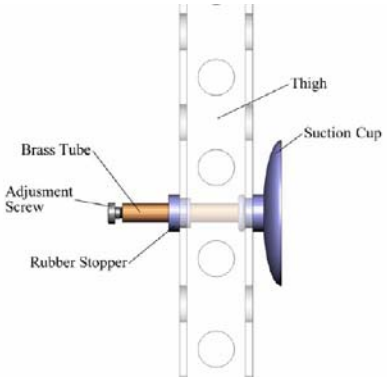

b) Knee Locking system

Fig.5: Knee Mechanism in Detail

4 Dynamics Algorithm

The Newton-Euler equation has been used to obtain the equations of motion of this model and will yield the following equations, after some rearrangements:

$$
\begin{aligned}
{}^{i+1}\omega_{i+1} &= {}^{i+1}_{i}R\,{}^{i}\omega_i + \dot{\theta}_{i+1}\hat{z}_{i+1}\\
{}^{i+1}\dot{\omega}_{i+1} &= {}^{i+1}_{i}R\,{}^{i}\dot{\omega}_i + {}^{i+1}_{i}R\,{}^{i}\omega_i \times \dot{\theta}_{i+1}\hat{z}_{i+1} + \ddot{\theta}_{i+1}\hat{z}_{i+1}\\
{}^{i+1}v_{i+1} &= {}^{i+1}_{i}R\left({}^{i}\omega_i \times {}^{i}p_{i+1} + {}^{i}v_i\right)\\
{}^{i+1}v^{c}_{i+1} &= {}^{i+1}\omega_{i+1} \times {}^{i+1}p^{c}_{i+1} + {}^{i+1}v_{i+1}\\
{}^{i+1}\dot{v}_{i+1} &= {}^{i+1}_{i}R\left({}^{i}\dot{\omega}_i \times {}^{i}p_{i+1} + {}^{i}\omega_i \times ({}^{i}\omega_i \times {}^{i}p_{i+1}) + {}^{i}\dot{v}_i\right)\\
{}^{i+1}\dot{v}^{c}_{i+1} &= {}^{i+1}\dot{\omega}_{i+1} \times {}^{i+1}p^{c}_{i+1} + {}^{i+1}\omega_{i+1} \times ({}^{i+1}\omega_{i+1} \times {}^{i+1}p^{c}_{i+1}) + {}^{i+1}\dot{v}_{i+1}
\end{aligned}
\qquad (1)
$$

Above, ${}^{i}\omega_i$ is the angular velocity of links and ${}^{i}\dot{\omega}_i$ is the angular acceleration of links. Also $(V,\dot{V})$ are the velocity and acceleration of each frame and $(V^c,\dot{V}^c)$ are the velocity and acceleration of center of mass of each link.

"Inertial forces" **F** and "Inertial torques" **N** are then defined for each link, (in terms of the θ_i, $\dot{\theta}_i$, and $\ddot{\theta}_i$);

$$
\begin{aligned}
{}^{i+1}F_{i+1} &= m_{i+1}\,{}^{i+1}\dot{v}^{c}_{i+1}\\
{}^{i+1}N_{i+1} &= {}^{i+1}I^{c}_{i+1}\,{}^{i+1}\dot{\omega}_{i+1} + {}^{i+1}\omega_{i+1} \times {}^{i+1}I^{c}_{i+1}\,{}^{i+1}\omega_{i+1}
\end{aligned}
\qquad (2)
$$

The effect of gravity is included most simply by accelerating the base of the mechanism ${}^{0}\dot{v}_0$ upward by g, and so one does not need to compute the forces and torques due to gravity in the equations above [1].
The acceleration of frame "0" is non-zero in general and is denoted by ${}^{0}\dot{v}_0$ and for ${}^{1}\dot{v}_1$ is modified in the above algorithm as follows.

$$
{}^{0}\dot{\mathbf{v}}_0 = \left[\mathbf{g}\cos\gamma, \quad R\ddot{\theta}_1 - \mathbf{g}\sin\gamma, \quad 0\right] \qquad (3)
$$

Here *R* is the radius of foot, $g\cos\gamma$ and $-g\sin\gamma$ terms result from accelerating the base upwards to account for the effect of gravity, as described above [4].

4.1 The Collision Dynamics

As mentioned before, the cycle of step starts after the heel strike and it lasts till the supporting leg converts to the swing leg. The motion equation in the 3 links state includes the walker's motion to the knee strike. Assuming the collision is ideal, which means there's no elastic motion in the collision, completing the motion, the state space should be gained according to the pre-collision parameters, exactly after the knee strike. Also the equations of motion for 2-link state include the walker's motion to the heel strike.
It is assumed that there has happened no elastic motion and also there is no collision between the previous supporting leg and the slope. Thus it is

possible to find the state space exactly after the heel strike and the knee strike according to the previous state space parameters, so the cycle will be completed [5].

The state space before the knee strike can be shown as $\{\theta_{st}^-, \theta_{th}^-, \theta_{sh}^-, \dot{\theta}_{st}^-, \dot{\theta}_{th}^-, \dot{\theta}_{sh}^-\}$. The sign "-" means they are related to the pre-collision moment.

Exactly after the knee strike, the state space including the supporting leg's angle θ_{st}^+, the swing leg's angle θ_{sw}^+ (or θ_{th}^+) and their relative velocities.

Although the post-collision state space is unknown, the relation between the angles for the shown model in fig 1 is as below:

$$\begin{aligned} \theta_{st}^+ &= \theta_{st}^- \\ \theta_{sw}^+ &= \theta_{th}^- = \theta_{th}^+ \end{aligned} \qquad (4)$$

As the angular momentum for the whole walker relative to the contact point of the supporting leg $\left(\mathbf{H}_{tot/cp}^- = \mathbf{H}_{tot/cp}^+\right)$, and for the swing leg relative to the thigh joint $\left(\mathbf{H}_{sw/h}^- = \mathbf{H}_{sw/h}^+\right)$ are constant in the collision, $\dot{\theta}_{st}^+$ and $\dot{\theta}_{sw}^+$ can be easily found, according to obtain the relation between the angular velocities.

Exactly before the heel strike, the state space includes the supporting leg angle θ_{st}^-, swing leg angle θ_{sw}^- and their relative velocities.

Exactly after the heel strike, the state space includes the supporting leg angle θ_{st}^+, swing leg angle θ_{th}^+ and their relative velocities. The relation between the angles is as below:

$$\begin{aligned} \theta_{st}^+ &= -\theta_{st}^- \\ \theta_{th}^+ &= -\theta_{sw}^- \\ \theta_{sh}^+ &= -\theta_{sw}^- = \theta_{th}^+ \end{aligned} \qquad (5)$$

Coming facts are used to find the angular velocities as before:

The angular momentum at the collision for the entire walker relative to the new contact point $\left(H_{tot/cp}^- = H_{tot/cp}^+\right)$, for the new swing leg relative to the thigh joint $\left(H_{sw/h}^- = H_{sw/h}^+\right)$ and for the new swing leg relative to the new swing knee $\left(H_{sh/k}^- = H_{sh/k}^+\right)$ will be constant.

In the 2-D state at the heel strike, 3 equations can be written for the angular momentum where solving them will lead to find the unknown parameters of $\dot{\theta}_{st}^+$, $\dot{\theta}_{th}^+$, $\dot{\theta}_{sh}^+$ in respect to the pre-collision parameters. For this purpose applying the analytic dynamic equations and according to the equations 1 to 5 and the on-line analyzing of it, all the necessary parameters can be found including $\dot{\theta}_{st}^+$, $\dot{\theta}_{th}^+$, $\dot{\theta}_{sh}^+$.

The smooth ODEs are generally integrated forward in time until the state vector approaches some collision condition which can be written as

$$h(\theta) = 0 \qquad (6)$$

Here $h(\theta)$ is a scalar function of the state. Approaching heelstrike, the function $h(\theta)$ often corresponds to the swing foot height above the ground. Approaching kneestrike, $h(\theta)$ corresponds to the difference between the swing knee angle and the locked knee angle.

5 Image Processing

Image processing is applied to obtain $\theta_{st}, \theta_{sh}, \theta_{sw}$. The most important advantage of such process is that the measuring tool has no effect on the measured object. Fast set up and to be independent from any other hardware are some other advantages of the process. Image processing is done with a PC and DSP is not used, because the digital signal processing (DSP) has a less processing rate. The image is taken by a CCD sensor with the resolution of (640x480). The modular design is presented in Fig.6.

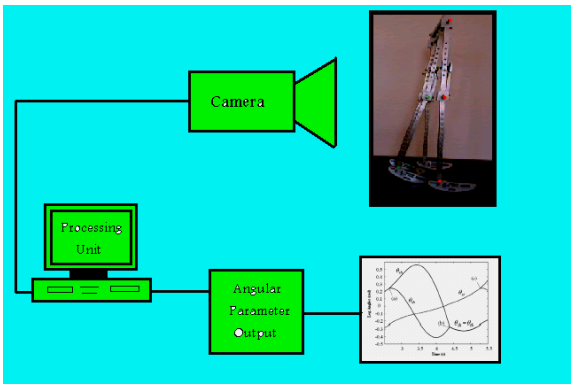

Fig.6: The modular

The purpose of image processing is to find the position of colored nodes as it is shown in Fig.7. Several frames are taken while the robot is moving and they will be processed later, because the time needed for saving the frames is less than time needed to process them. By this method θ can be found precisely.

5.1 Process Algorithm

Fig.7 shows a linear system model of a typical digital image processing system.

Transfer function of each component can be modeled analytically, determined experimentally, or

taken from manufacturer's specifications. The lenses, for example, can be assumed diffraction limited.
The computer operation may or may not be linear, but this is the only subsystem in fig-1that is directly under the user's control [10].

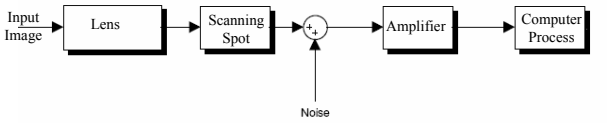

Fig.7: The elements of an image processing system

The plane coordinate is divided to 3 geometrical zones and also 2 color zones. All zones should be distinguished from each other. The geometrical and color zones, is shown in Fig.9.

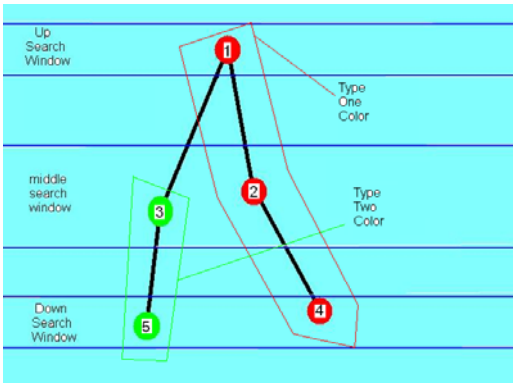

Fig.8: Geometric and color zone

The amounts of the position areas are given to the image process program. According to process two different colored areas it is not possible to use hardware filters, so the RGB (Red, Green, and Blue) software filters are used.
Each of the amounts of R, G and B for a singular pixel can be in the range of 0 and 255.
In the beginning the program appropriate amounts of the filter parameters and their application must be given to the program according to a sample frame. For example to identify the yellow color the amounts of the R and G must be more than 200 and amount of B must be less than 150. Thus the program has to find the desired color in different areas. The color space of this process is shown Fig.9. According to the separating method of the position areas and colored areas, it is assured that the obtained point is unique.

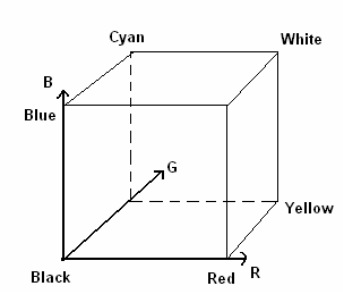

Fig.9: Rectangular color space

As the relation of the distance between the planes - where the nodes are inside them – and the mean distance of them to camera is very close to **1**, all the nodes can be assumed in the same plane. It is due to the effect of immeasurable factors on the transfer function of the pixel positions to the real positions.
Finally, by having the nodes positions and the amount of frames per second it is possible to compute the θ and $\dot{\theta}$.
In cases where the mid-legs is covered by the leg that is faced to the camera - which prevents it to find the nodes- Linear Regression method is used to obtain closest datum to the unknown data.
For obtaining angular velocity and acceleration the following formulation (5 points differential) is used:

$$f'(x_0) = h/12[-25f(x_0) + 48f(x_0 + h) - 36f(x_0 + 2h) + 16f(x_0 + 3h) - 3f(x_0 + 4h)] \quad (6)$$

To install the program, Delphi 7.0 is used. The GUI program is shown in Fig.9.

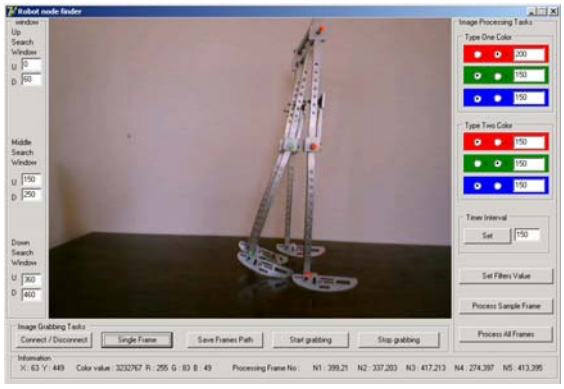

Fig9: The GUI Program under Delphi 7.0

6 Results

To obtain an appropriate cycle of the movement the physical parameters of the model have a certain role. These parameters are shown in Figure (1). Some of this parameter such as the length of the legs and the radius of the sole are constant, but other parameters are changeable. For this purpose, the

position of the center of mass and the gyration radius can be changed by increasing the mass.
Applying this method on the manufactured prototype, the appropriate amounts of these parameters found after several tests.
They are presented in Table 1. The physical parameters of the walker are presented in Table 2.

Table 1: The changed parameters in the test

Model	$m_t,(kg)$	$r_t,(m)$	$c_t,(m)$
A	0.9643	0.14	0.11
B	1.5643	0.102	0.112
C	1.9543	0.0995	0.105
Final	2.4443	0.0995	0.091

Table 2 : The physical Parameters of the model

l_t	0.35m	m_s	1.015m
w_t	0m	r_s	0.197m
m_t	2.4443kg	c_s	0.17m
r_t	0.0995	R	0.2m
c_t	0.091m	γ	0.036rad
l_s	0.45m	g	m/s^2 9.81
w_s	0.03kg	ε_T	0.097rad

The period of each step cycle is obtained 3 seconds. The Leg angles are taken from image processor for 5 levels of the movement and are compared with the numerical results which are taken from the numerical simulation. They are presented in the following table.

Table 3 - Numerical and Experimental Leg angles

	Numerical (rad)			Experimental (rad)		
Time (s)	θ_{st}	θ_{th}	θ_{sh}	θ_{st}	θ_{th}	θ_{sh}
2.25	-0.2439	0.2439	0.2439	-0.2439	0.2439	0.2439
3	-0.1654	0.1423	0.4253	-0.1726	0.1521	0.4355
3.75	-0.0895	-0.3325	0.4925	-0.0912	-0.3565	0.4525
4.5	0.0485	-0.2935	-0.2935	0.0435	-0.2785	-0.2785
5.25	0.2439	-0.2439	-0.2439	0.2439	-0.2439	-0.2439

The curves of the angles of $\theta_{st},\theta_{sh},\theta_{sw}$ are plotted in Diagram (1) where they are assumed as functions of time. The confliction points are highlighted in it. (a) is the heel strike point, (b) is Knee strike point and (c) is Heel strike again.

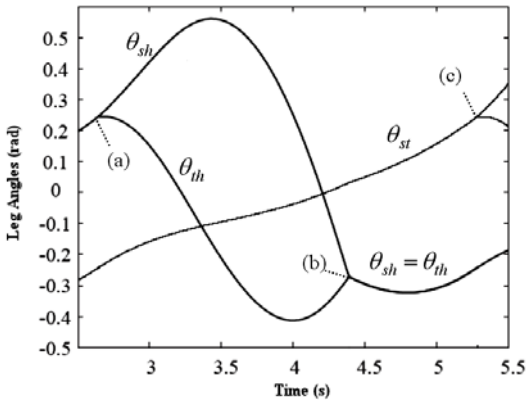

Diagram 1 - The Curves of Foot Angles (Rad) Respect to the Time (Sec)

According to the Diagram and the presented states, the area between (a) and (b) stands for the 3-link mode and (b) to (c) stands for 2-link mode.
Also, as it is expected after the knee strike, the angles of the thigh and the leg will be the same ($\theta_{th}=\theta_{sh}$) and will consist the swing leg's angle (θ_{sw}).
It should be mentioned that the parameters of table (2) are used in simulation and also the initial state space conditions for the best step cycle are as below based on the try and error method:

$$\begin{aligned}
&\theta_{st}(0) = -0.2439 rad \\
&\theta_{th}(0) = 0.2439 rad \\
&\theta_{sh}(0) = 0.2439 rad \\
&\dot{\theta}_{st}(0) = -1.049 rad/s \\
&\dot{\theta}_{th}(0) = 1.049 rad/s \\
&\dot{\theta}_{sh}(0) = 2.23 rad/s
\end{aligned} \qquad (6)$$

7 Conclusion

In this paper the specifications of the passive biped walkers are presented firstly, and the governing equations of them are explained. Then, by changing the physical parameters, the physical model is analyzed and the appropriate step cycle is obtained. Also the legs' angels for a step cycle simulated as a function of time.
For programming Delphi 7.0 is applied, where SolidWorks and Matlab were used for the designing and numerical simulation, respectively.

References:

1. T, McGeer, "Passive walking with knees", Proceeding of the IEEE Conference on Robotics and Automation, 2:1645-16451, 1997.

2. M, Garcia, A, Ruina, A, Chaterjee, “Efficiency and stability of 2-D passive dynamic kneed walking”, ICRA98, 1998.
3. M, Garcia, A, Ruina, A, Chaterjee, M, Coleman, “The simplest walking model: Stability, complexity, and scaling”, Accepted for publication in the ASME Journal of Biomechanical Engineering, 1997.
4. S, Collins, M, Wisse, A, Ruina, “A Three-Dimensional Passive-Dynamic Walking Robot with Two Legs and Knees”, The International Journal of Robotics Research, Vol. 20, No. 7, pp: 607-615, July 2001.
5. A, Ruina, “Nonlinear-Dynamic study of walking: simulation, analysis, and experiment. A research proposal submitted to the National Science Foundation, 1997.
6. M, Garcia, A, Ruina, A, Chaterjee, “Efficiency, Speed, and Scaling of 2D passive Dynamic Walking”, Submitted to Dynamic and Stability of Systems July 29, 1998.
7. M, Garcia, A, Ruina, A, Chaterjee, “Efficiency, Speed, and Scaling of Small-Slope 2-D passive Dynamic Bipedal Walking”, last revised version of Submitted to Dynamic and Stability of Systems, September, 1999.
8. M, Garcia, “Stability, Scaling and Chaos in Passive-Dynamic Gait Models”, A Dissertation Presented to the Faculty of the Graduated School of Cornell University, January 1999.
9. A. Hajiloo, " Design and Manufacturing of a Passive Biped Walker" , B.Sc. Dissertation, University of Guilan, 2004
10. Kenneth R. Castleman, Digital Image Processing, Prentice Hall, New Jersey, 1996